

Superconductivity in an Inorganic Electride $12\text{CaO}\cdot 7\text{Al}_2\text{O}_3\cdot e^-$

Masashi Miyakawa,[†] Sung Wng Kim,[†] Masahiro Hirano,[†] Yoshimitsu Kohama,[‡] Hitoshi Kawaji,[‡]
Tooru Atake,[‡] Hiroki Ikegami,[§] Kimitoshi Kono,[§] and Hideo Hosono^{*,†,‡}

Frontier Collaborative Research Center, Tokyo Institute of Technology, Mail Box S2-13, 4259 Nagatsuta, Midori-ku, Yokohama 226-8503, Japan, Materials and Structures Laboratory, Tokyo Institute of Technology, Mail Box R3-7, 4259 Nagatsuta, Midori-ku, Yokohama 226-8503, Japan, and Low Temperature Physics Laboratory, RIKEN, Hirosawa 2-1, Wako, Saitama 351-0198, Japan

Received April 9, 2007; E-mail: hosono@msl.titech.ac.jp

Representative metal oxides, such as Al_2O_3 and SiO_2 , are widely used as ingredients of architectural materials and optical components because they and their mixed compounds are most abundant in resource and are environmentally benign. However, almost no active electronic functions are possible to implement in these materials due mostly to difficulty in efficient carrier doping. Recently, high-electron-carrier doping to $12\text{CaO}\cdot 7\text{Al}_2\text{O}_3$ (C12A7) crystal has been realized by a chemical reduction treatment, in which oxygen ions in sub-nanometer-sized crystallographic cages are extracted selectively.^{1,2} Since the doped electron nominally occupies the former oxygen ion site and acts as an anion, the resultant compound may be regarded as a type of “electride”, which is composed of the anionic electron and the cationic framework.³

As a precursor of the electride, the C12A7 crystal is a compound in the system $\text{CaO}-\text{Al}_2\text{O}_3$ ⁴ and is used widely as a constituent of aluminous cements.⁵ The C12A7 exhibits totally different physical and chemical properties from the other compounds in this system. This is due mostly to its unique crystal structure (Figure 1).⁶ The unit cell containing two molecules of C12A7 is represented as $[\text{Ca}_{24}\text{Al}_{28}\text{O}_{64}]^{4+}(\text{O}^{2-})_2$. The first part denotes a positively charged framework constructed by 12 crystallographic cages with an inner diameter of ~ 0.4 nm, and the second part represents two extra framework oxygen ions entrapped in two different cages as counteranions (i.e., the remaining 10 cages are empty). They can be replaced with other anions such as OH^- and F^- .⁷ Further electrons can substitute totally and partially for them to form $[\text{Ca}_{24}\text{Al}_{28}\text{O}_{64}]^{4+} 2[(1-x)\text{O}^{2-} + 2x(e^-)]$, in which the maximum electron concentration ($2.3 \times 10^{21} \text{ cm}^{-3}$), corresponding to $x = 1$, is limited by the total positive charge of the framework.

In the preceding paper,² we reported that metal–insulator transition occurs in this material by doping electrons to $> 1 \times 10^{21} \text{ cm}^{-3}$, and its mechanism which is evidenced by detailed structural analysis is rather different from that reported in conventional semiconductors. Our next interest for this material is to examine whether superconducting transition occurs or not. No superconducting transition has been observed for representative metal oxides as well as electriles to date. In this study, we have measured electrical resistivity with and without an external magnetic field as well as magnetic susceptibility for both single crystals and thin films of the C12A7 electride ($12\text{CaO}\cdot 7\text{Al}_2\text{O}_3\cdot e^-$) down to 85 mK, finding that superconducting transition (T_c) has been clearly observed for all of the samples. The value of T_c varies in the range of 0.14–0.4 K with the concentration of anionic electrons (N_e).

Employed samples were nominally pure single-crystal⁸ (sc) and thin-film $12\text{CaO}\cdot 7\text{Al}_2\text{O}_3\cdot e^-$. The contamination of paramagnetic impurities

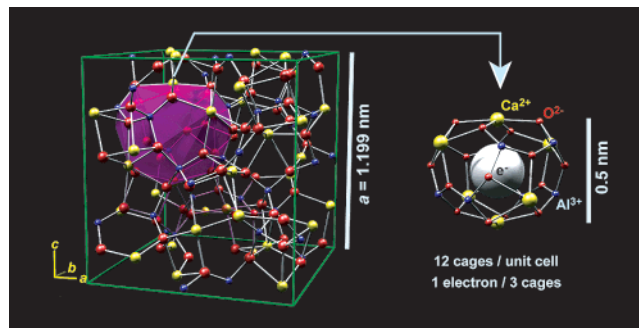


Figure 1. Crystal structure of the C12A7 electride $[\text{Ca}_{24}\text{Al}_{28}\text{O}_{64}]^{4+}(\text{e}^-)_4$ (left) and an extracted cage structure (right). Red, yellow, and blue balls represent oxygen, calcium, and aluminum atoms, respectively. Electrons in the cages are neglected for simplicity. The green box shows a cubic unit cell containing 12 cages, and one of the cages is marked by purple color. Each cage has a free space with an inner diameter of ~ 0.4 nm. Electron occupancy of the cage is $4/12$.

in the samples was carefully avoided because these ions may induce a Kondo effect.⁹ The sc-C12A7: e^- was prepared by a reduction treatment using Ti metal.² After the reduction treatments, sample surfaces were mechanically polished to remove the Ti-related compounds. It was confirmed by X-ray diffraction that neither metallic Ti nor Ti suboxide layers remain on the sample surface. Further, the crystal framework structure remains unchanged by this treatment. The bulk sc-C12A7: e^- looked black and exhibited metallic conduction with a conductivity of ~ 810 (sample A, dimension $\sim 4 \times 15 \times 2 \text{ mm}^3$) and $\sim 770 \text{ S}\cdot\text{cm}^{-1}$ (sample B, $\sim 2 \times 6 \times 1 \text{ mm}^3$) at 300 K. The thin films of $12\text{CaO}\cdot 7\text{Al}_2\text{O}_3\cdot e^-$ were fabricated by a reduction of a C12A7 film on $\text{Y}_3\text{Al}_5\text{O}_{12}$ (YAG) substrate through a two-step C12A7 film deposition process.¹⁰ A cross-sectional image of a transmission electron microscopy and an electron diffraction pattern of the electride film showed that the film was oriented to the substrate with an orientation relationship of $\text{C12A7}(001) \parallel \text{YAG}(001)$ and $\text{C12A7}[100] \parallel \text{YAG}[100]$. The whole area of the film on the YAG substrate was not completely oriented but contained a few domains with different orientations. $12\text{CaO}\cdot 7\text{Al}_2\text{O}_3\cdot e^-$ films with different thicknesses of ~ 245 (sample C) and ~ 150 nm (D) were employed for further measurements. Both films showed metallic conduction with ~ 310 and $\sim 560 \text{ S}\cdot\text{cm}^{-1}$ at 300 K, respectively. The carrier concentrations in the films evaluated by Hall voltage measurements were $\sim 1.6 \times 10^{21} \text{ cm}^{-3}$ for sample C and $\sim 2.0 \times 10^{21} \text{ cm}^{-3}$ for sample D. The averaged internal transmission in the visible light region (400–800 nm) of sample C (245 nm) is $\sim 59\%$, and accordingly, the film looks brown but transparent. This good transparency results from specific electronic nature¹¹ of the $12\text{CaO}\cdot 7\text{Al}_2\text{O}_3\cdot e^-$, that is, the low N_e ($1-2 \times 10^{21} \text{ cm}^{-3}$) and the smaller effective mass ($0.82m_e$)¹⁰ yield the major part of the free carrier absorption in the near-infrared region.

[†] Frontier Collaborative Research Center, Tokyo Institute of Technology.

[‡] Materials and Structures Laboratory, Tokyo Institute of Technology.

[§] Low Temperature Physics Laboratory, RIKEN.

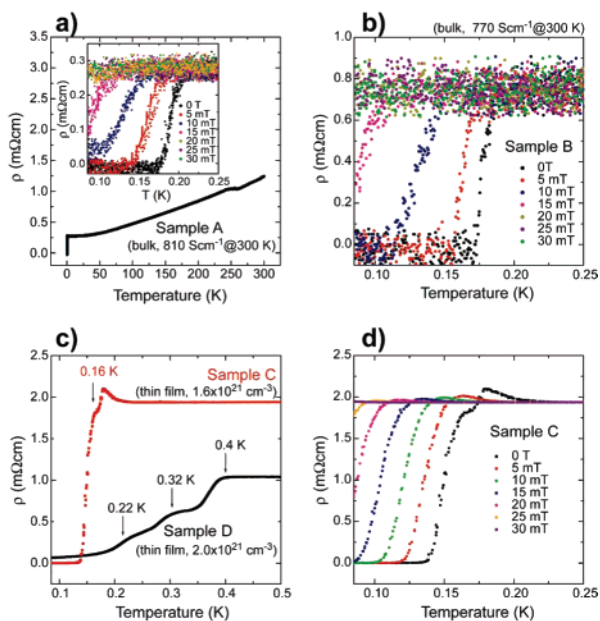


Figure 2. Electrical and magnetic properties of C12A7 electride single crystals and thin films. (a) Temperature dependence of the electrical resistivity (ρ) of the single crystal C12A7 electride (sample A). Inset is ρ - T curves at low temperatures for magnetic fields at 0, 5, 10, 15, 20, 25, and 30 mT. (b) ρ - T curves of sample B at low temperatures for magnetic fields from 0 to 30 mT. The poor S/N resolution for the bulk samples is due to experimental limitation; that is, a small current is needed to suppress Joule heating, leading to the shift of T_c . (c) ρ - T curves for C12A7 electride thin films on YAG substrate (samples C and D) at low temperatures. (d) ρ - T curves of sample C for several external magnetic fields from 0 to 30 mT.

The electrical resistivity measurement was performed by a standard four-probe method using Pt electrodes. Figure 2a shows temperature (T) dependence of the electrical resistivity (ρ) of sample A. The inset of Figure 2a represents expanded ρ - T curves (for sample A) below 0.25 K for various external magnetic fields. A sharp drop of the resistivity is observed with an onset temperature of ~ 0.2 K, and the resistivity becomes an immeasurably small value below 0.17 K. It also confirms for sample B (Figure 2b). Further, the onset temperature decreases with the application of magnetic field. These observations strongly suggest that sc-C12A7:e⁻ is a superconductor below a T_c of ~ 0.2 K, and the superconductivity is destroyed by the magnetic field above a critical magnetic field of 30 mT.

A similar sharp drop in ρ - T curves was observed with the onset temperature of ~ 0.16 K in sample C, and the drop in sample D took place in three steps with onset temperatures of ~ 0.4 , ~ 0.32 , and ~ 0.22 K (Figure 2c). The drop in sample C shifts to lower temperature with the magnetic field (Figure 2d). Thus, the sharp drops in the thin-film samples are attributed to the transition from normal to superconductive state as in the bulk samples. The three-step drop in sample D suggests that T_c depends on the N_e , and the film is nonuniform with respect to the N_e . Since the average carrier concentration of sample D ($2.0 \times 10^{21} \text{ cm}^{-3}$) is higher than that of sample C ($1.6 \times 10^{21} \text{ cm}^{-3}$), it appears that T_c increases with the N_e .

The measurement of an ac magnetic susceptibility (χ) of samples A and B was performed from the change in the mutual inductance between two small coils at 120 Hz in a dilution refrigerator. The absolute value (included $\pm 5\%$ error) of χ was calibrated from

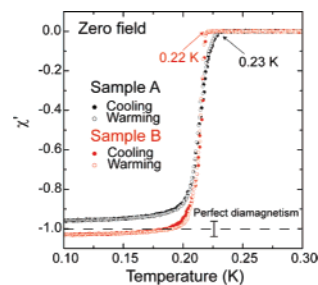


Figure 3. Real part of ac magnetic susceptibility of single crystal C12A7 electride (samples A and B) near superconducting transition temperature.

perfect diamagnetisms of Al and Ti metals. Figure 3 shows the real part of the ac magnetic susceptibility of samples A and B as a function of temperature. The χ - T curves for zero field cooling and warming do not differ significantly. The observation of a sharp drop and perfect diamagnetism ($\chi \approx -1$) below 0.20 K in the χ - T curve confirms the bulk superconductivity in the C12A7:e⁻. A broader transition region was observed in the sample A. This is due probably to the larger inhomogeneity of local carrier density arising from larger sample dimension. The onset temperature in the ρ - T curve is slightly lower than that in the χ - T curve, which is attributed to Joule heat unavoidably generated in the electrical resistivity measurement that induced possible temperature gradient between the sample and the temperature-monitoring point. The critical magnetic field $H_c(0)$ is estimated to be ~ 19 mT for the bulk and ~ 33 mT for the thin film using a relation of $H_c(T) = H_c(0)[1 - (T/T_c)^2]$.

In summary, zero resistivity, magnetic field-dependent resistance, and perfect diamagnetism indicate that the representative metal oxide based C12A7:e⁻ is a superconductor with a T_c of ~ 0.4 K, which depends on the anionic electron concentration. Most carrier electrons are populated in the free space inside the crystal lattice. Such a situation is a striking difference from that in other superconductors/metals. Thus, the present finding of the superconductivity in the C12A7:e⁻ implies that the “electride” is a promising material category for realizing an exotic superconductor.

Supporting Information Available: Experimental details, TEM, and optical data. This material is available free of charge via the Internet at <http://pubs.acs.org>.

References

- (1) Matsuishi, S.; Toda, Y.; Miyakawa, M.; Hayashi, K.; Kamiya, T.; Hirano, M.; Tanaka, I.; Hosono, H. *Science* **2003**, *301*, 626.
- (2) Kim, S. W.; Matsuishi, S.; Nomura, T.; Kubota, Y.; Takata, M.; Hayashi, K.; Kamiya, T.; Hirano, M.; Hosono, H. *Nano Lett.* **2007**, *7*, 1138.
- (3) (a) Dye, J. L. *Inorg. Chem.* **1997**, *36*, 3816. (b) Dye, J. L.; Wagner, M. J.; Overny, G.; Huang, R. H.; Nagy, T. F.; Tomanek, D. *J. Am. Chem. Soc.* **1996**, *118*, 7329. (c) Ichimura, A. S.; Dye, J. L.; Cambor, M. A.; Villaescusa, L. A. *J. Am. Chem. Soc.* **2002**, *124*, 1170.
- (4) Chatterjee, A. K.; Zhmoidin, G. I. *J. Mater. Sci.* **1972**, *7*, 93.
- (5) Taylor, H. F. W. *Cement Chemistry*, 2nd ed.; Thomas Telford: London, 1997.
- (6) Scheller, H. B. T. *Neues Jahrb. Mineral. Monatsh.* **1970**, *35*, 547.
- (7) (a) Imlach, J. A.; Glasser, L. S. D.; Glasser, F. P. *Cement Conc. Res.* **1971**, *1*, 57. (b) Jeevaratnam, J.; Glasser, F. P.; Glasser, L. S. D. *J. Am. Ceram. Soc.* **1964**, *47*, 105.
- (8) Watauchi, S.; Tanaka, I.; Hayashi, K.; Hirano, M.; Hosono, H. *J. Cryst. Growth* **2002**, *237*–239, 496.
- (9) Kondo, J. *Solid State Phys.* **1969**, *23*, 183.
- (10) Miyakawa, M.; Kamiya, T.; Hirano, M.; Hosono, H. *Appl. Phys. Lett.* **2007**, *90*, 182105.
- (11) (a) Sushko, P. V.; Shluger, A. L.; Hirano, M.; Hosono, H. *J. Am. Chem. Soc.* **2007**, *129*, 942. (b) Sushko, P. V.; Shluger, A. L.; Hayashi, K.; Hirano, M.; Hosono, H. *Phys. Rev. Lett.* **2003**, *91*, 126401.

JA0724644